HHS Public Access

Author manuscript

ACS Infect Dis. Author manuscript; available in PMC 2017 April 08.

Published in final edited form as:

ACS Infect Dis. 2016 April 8; 2(4): 281–293. doi:10.1021/acsinfecdis.5b00143.

High-Throughput Luciferase-Based Assay for the Discovery of Therapeutics That Prevent Malaria

Justine Swann[1], **Victoria Corey**[1], **Christina A. Scherer**[2], **Nobutaka Kato**[2], **Eamon Comer**[2], **Micah Maetani**[2], **Yevgeniya Antonova-Koch**[1], **Christin Reimer**[1], **Kerstin Gagaring**[3,&], **Maureen Ibanez**[3,%], **David Plouffe**[3], **Anne-Marie Zeeman**[4], **Clemens H. M. Kocken**[4], **Case W. McNamara**[2,&], **Stuart L. Schreiber**[2], **Brice Campo**[5], **Elizabeth A. Winzeler**[1], and **Stephan Meister**[1,#]

[1]University of California, San Diego (UCSD), School of Medicine, Dept. Pediatrics, Pharmacology & Drug Discovery, 9500 Gilman Drive, La Jolla, CA 92093, USA [2]The Broad Institute, 415 Main Street, Cambridge, MA 02142, USA [3]Genomics Institute of the Novartis Research Foundation (GNF), 10675 John Jay Hopkins Drive, San Diego, CA 92121, USA [4]Department of Parasitology, Biomedical Primate Research Centre, PO Box 3306, 2280 GH Rijswijk, The Netherlands [5]Medicines for Malaria Venture (MMV), Meyrin 2015, Switzerland

Abstract

In order to identify the most attractive starting points for drugs that can be used to prevent malaria, a diverse chemical space comprising tens of thousands to millions of small molecules may need to be examined. Achieving this throughput necessitates the development of efficient ultra-high-throughput screening methods. Here, we report the development and evaluation of a luciferase-based phenotypic screen of malaria exoerythrocytic-stage parasites optimized for a 1536-well format. This assay uses the exoerythrocytic-stage of the rodent malaria parasite, *Plasmodium berghei,* and a human hepatoma cell line. We use this assay to evaluate several biased and unbiased compound libraries, including two small sets of molecules (400 and 89 compounds, respectively) with known activity against malaria erythrocytic-stage parasites and a set of 9,886 Diversity-Oriented Synthesis (DOS)-derived compounds. Of the compounds screened we obtain hit rates of

[#]Correspondence to ; Email: smeister@ucsd.edu
[&]Present address: California Institute for Biomedical Research (Calibr), San Diego, CA 92037, USA
[%]present address: Samumed, San Diego, CA 92121, USA

Author Contributions

EAW wrote the manuscript and analyzed data. SM performed assays, analyzed data and wrote the manuscript. JS wrote the manuscript, analyzed data, performed flow cytometry and time of action assays. VC analyzed data and created figures. CAS wrote the manuscript, created figures and provided compounds. NK performed erythrocytic-stage screens. EC and MM analyzed data. CWM provided advice. DP performed assays and optimization. CR performed assays and wrote the manuscript. YAK, SK, KH, and MI performed assays. SLS wrote the manuscript. AMZ and CHMK performed *P. cynomolgi* assays. BC provided advice and wrote the manuscript.

Supporting information

As supporting information, we have included a illustrating results obtained during the optimization of the high-throughput luciferase assay, figures graphically illustrating compound hit selection from both the MMV Malaria Box screen and the Broad DOS screen, and a figure displaying IC_{50} and CC_{50} curves for selected MMV Malaria Box hits in two hepatocyte cell lines. We also include a table reporting the IC50 data for the validation set of antimalarials, and two spreadsheets with the detailed results from the MMV Malaria Box and Broad DOS library screens. This information is available free of charge via the Internet at https://www.ebi.ac.uk/chemblntd (Set 18).

12–13% and 0.6% in preselected and naïve libraries, respectively, and identify 52 compounds with exoerythrocytic-stage activity less than 1 μM, and having minimal host cell toxicity. Our data demonstrate the ability of this method to identify compounds known to have causal prophylactic activity in both human and animal models of malaria, as well as novel compounds, including some exclusively active against parasite exoerythrocytic stages.

Keywords

Malaria; drug discovery; high-throughput screening; exoerythrocytic-stage malaria; liver-stage malaria

Introduction

Despite being an ancient disease, malaria is still responsible for over a half million deaths and substantial morbidity, poverty, and suffering for hundreds of millions of people each year[1–3]. It is a vector-borne disease caused by infection with *Plasmodium* parasites transmitted through the bite of *Anopheles* mosquitoes. While eradication campaigns have been successful in most of North America and Europe, malaria continues to devastate developing regions of Asia, Africa, and South America[4]. The mortality rates are highest amongst African children, with an estimated one death per minute (WHO). The emergence of resistance to all of the current frontline antimalarial drugs warrants global concern[5]. It is therefore critical that new drugs are developed that not only treat disease symptoms, but also contribute towards the elimination and eradication of malaria infections. In order to achieve eradication, new drugs should inhibit multiple developmental stages of the parasite. Following the blood meal of an infected *Anopheles* mosquito, *Plasmodium* sporozoites travel through the bloodstream to reach the liver. The sporozoites traverse multiple cells within the liver before establishing productive invasion within hepatocytes, where they transform into exoerythrocytic-stage exoerythrocytic forms (EEFs)[6]. Depending on the species, these exoerythrocytic forms enter one of two developmental pathways: they can form mature exoerythrocytic-stage schizonts, or they can enter a dormant phase called hypnozoites. The determinant factors guiding exoerythrocytic-stage development towards hypnozoite formation in *P. vivax* and *P. ovale* are not understood. Hypnozoites can reinitiate development and give rise to malaria relapses weeks, months or even years after the initial infection[7]. Fully developed exoerythrocytic-stage merozoites within schizonts eventually egress from the liver and re-enter the bloodstream[6]. The continuous replication of asexual bloodstages within red blood cells (RBCs) causes RBC destruction and leads to the characteristic symptoms associated with malaria: anemia, fever and chills[8]. A small percentage of these asexual-blood stage parasites will then differentiate into sexual erythrocytic-stage parasites as female and male gametocytes, and the transmission of the sexual blood stage back to the mosquito vector during a subsequent blood meal completes the life cycle[9].

The majority of the current antimalarials only treat the symptom-causing erythrocytic stages of the parasite[10]. A few classes, including cytochrome bc1 inhibitors (such as atovaquone) and antifolate drugs (such as pyrimethamine), are active against developing exoerythrocytic

forms as well as erythrocytic forms and are able to prevent the establishment of infection (causal prophylactic activity) as well as relieve symptoms[10]. Antibiotics, such as doxyclycline, clindamycin, and azithromycin, are also an important class of antimalarial drugs. Doxyclycline is commonly prescribed to travelers to endemic areas and is especially useful for its casual prophylaxis and slow acting blood schizontocidal activity[11]. The 8-aminoquinolines (such as primaquine and tafenoquine) are a unique class in that they can eliminate hypnozoites as well and can provide a radical cure for *P. vivax* and *P. ovale*[7, 10]. Having new classes of drugs that could be used prophylactically and/or to provide a radical cure would be desirable. Resistance is developing to both napthoquinones and antifolates, and 8-aminoquinolines can be toxic to individuals with glucose-6-phosphate deficiency[10, 12]. Drugs targeting the exoerythrocytic-stage only would also offer the reduced potential for drug resistance, as there are far fewer parasites at this 'bottleneck' compared to the replicative erythrocytic stages[10]. Accordingly, the development of an exoerythrocytic-stage specific high-throughput screening assay is necessary in order to identify the next generation of antimalarial drugs.

Although it is possible to create new chemical derivatives of existing drugs with improved therapeutic and resistance profiles, phenotypic screening offers the opportunity to find entirely new classes of small molecules that are active against exoerythrocytic stages of the life-cycle(13). We have previously reported an immunofluorescence-based malaria exoerythrocytic-stage assay that we used to screen a library of >4,000 commercially available compounds with erythrocytic-stage activity(14). While this platform led to the identification of 275 exoerythrocytic-stage active compounds, the assay is limited to a 384-well throughput and is therefore not suitable for the screening of larger chemical libraries, in part because of the high cost of sporozoites obtained by manual mosquito dissections ($1.00 per well screened). In addition, the requirement for a specialized high-content imaging device limits the accessibility of the assay. Other malaria exoerythrocytic-stage drug screens have utilized *P. berghei* sporozoites that express a luciferase reporter (Pb-Luc)(15, 16),(17) however, these assays are also limited by a 384-well assay throughput. In this report, we describe the development of a high-throughput luciferase-based assay that can be used to screen chemical libraries in a 1536-well plate format. We demonstrate that the assay is highly sensitive, reproducible, and efficient. As proof of concept, we use this assay to screen the Medicines for Malaria Venture (MMV) Malaria Box for compounds with exoerythrocytic-stage activity(18) as well as a larger collection of chemical compounds from the Broad Diversity-Oriented Synthesis Library, a set that includes compounds with and without demonstrated erythrocytic-stage antimalarial activity.

Results and Discussion

Development of a luciferase-based high-throughput exoerythrocytic-stage assay

In order to develop a high-throughput exoerythrocytic-stage malaria assay capable of screening large libraries of chemical compounds, a number of tests were performed to optimize a 48 hour *in vitro* PbGFP-Luc-SM_{CON}[19] infection of HepG2-A16-$CD81^{EGFP}$ hepatocytes[20] (Figure S1). This rodent *Plasmodium* strain was previously generated through the integration of a GFP-Luc cassette into the *c-rrna* locus and selecting transgenic

P. berghei by flow sorting GFP-expressing parasites. For simplicity, we will refer to this strain as Pb-Luc. For these tests, HepG2-A16-CD81^{EGFP} cells were seeded in 1536-well plates 24 hours prior to infection and luciferase bioluminescence measured 48 hours post infection to detect parasite viability. We found the ideal ratio of sporozoites to cells per well to be 1:3, respectively (1×10^3 sporozoites in 5 μl to 3×10^3 cells in 5 μl) (Figure 1A, Figure S1A). At these concentrations, the cells were ideally confluent and the infection rate produced luciferase values that were significantly greater than background values at 48 hours post infection (Figure S1A). Furthermore, tests without hepatocytes showed that there was no residual luciferase activity from Pb-Luc sporozoites at 24 hours post infection at 37°C (Figure S1B), eliminating the possibility that sporozoites which had not invaded contribute to the luciferase signal. We also tested different DMSO concentrations (added 18 hours pre-infection) to assess their impact on parasite viability, and found that concentrations up to 0.88% DMSO had an insignificant effect on luciferase activity 48 hours post infection (Figure S1C). The final protocol was to add 50 nl of compound in DMSO (resulting in 50 μM compound and 0.5% DMSO concentration in the assay plates) 18 hours pre-infection in the optimized screening assay (Figure 1A). An example of the luciferase signal for two replicate plates seeded with a representative small molecule library is shown in Figure 1B. Z factor for these plates was between 0.7 and 0.9, an excellent value for a phenotypic screen.

Assay validation through screening of known antimalarial compounds

To validate this assay further, we next examined several compound collections. We first evaluated 50 established antimalarial clinical or tool compounds (Table S1) that have been tested in other antimalarial phenotypic assays[10]. The most active compounds included the electron transport chain inhibitor atovaquone, antifolate pathway inhibitors P218•HCl, pyrimethamine and cycloguanil, the protein biosynthesis inhibitor cycloheximide, and the glutathione reductase inhibitor methylene blue. For these compounds, the exoerythrocytic-stage half maximal inhibitory concentration (IC_{50}) values were similar to the *P. falciparum* erythrocytic-stage IC_{50} values. Compounds that were less active relative to erythrocytic-stages, on the other hand, included 4-aminoquinolines, amino alcohols, and endoperoxides, which presumably act primarily against hemoglobin degradation, a process that does not occur during hepatic stages. Overall, these results were highly consistent with our previously established high-content imaging (HCI) assay of the hepatic stages against the related rodent parasite, *Plasmodium yoelii*[10].

For active compounds, we also compared the IC_{50} values for Pb-Luc generated by the luciferase-based enzymatic assay to values produced by screening Pb-Luc parasites using our previously established (HCI) assay that uses polyclonal *Plasmodium* HSP70 antibody staining at 48 hours as an indicator of infection[14] (Figure 2). We found that there was a strong correlation between compound activities in both assays, as indicated by an R^2 of 0.83, but the high-throughput luciferase-based assay resulted in IC_{50}s roughly 10× lower (Figure 2). Since luciferase is relatively unstable, with a half-life of less than 2 hours [21], this may lead to a higher rate of reporter turnover and therefore increased sensitivity to compounds that inhibit parasite growth at later stages compared to that of parasite HSP70 (as measured

in the HCI assay). Additionally, non-viable parasites may be stained using the HCI assay, whereas they may not produce luciferase.

Screening the MMV Malaria Box for exoerythrocytic-stage inhibitors

After establishing the high-throughput luciferase-based assay quality, reproducibility, and sensitivity, we sought to test its validity as a platform to screen diverse chemical libraries by screening the MMV Malaria Box[18]. This open-access set consists of 400 compounds that were selected from a group of ~20,000 antimalarial hits generated from a large-scale erythrocytic-stage screening of >4,000,000 compounds by St. Jude Children's Hospital, Novartis, and GSK (Figure S2). The library contains 200 'probe-like' and 200 'drug-like' compounds, selected based on their chemical diversity, erythrocytic-stage antimalarial activity, and commercial availability. The Malaria Box compounds have erythrocytic-stage activity ranging from an IC_{50} of 30 nM to 4 μM[18]. Compounds originating in the Novartis collection had been previously tested in the *P. yoelii* assay[14] but others had not, providing valuable internal controls.

After a first-round screening of the MMV Malaria Box at compound concentrations of 50 μM in duplicate plates, 48 compounds were selected for reconfirmation based on Pb-Luc inhibition of more than 90% and HepG2 cytotoxicity of less than 25% in both assay plates, a hit rate of 12%. These were tested in a 12-point serial dilution dose response beginning at 10 μM. Of those retested, 36 had a Pb-Luc IC_{50} < 10 μM and counter-screening for HepG2 cytotoxicity and luciferase inhibition produced IC_{50} values greater than 10 μM (Figure 3, see Additional File 1 for full screening results), leading to a confirmation rate of 75%. Furthermore, more than half of these compounds were very active against Pb-Luc exoerythrocytic-stages with IC_{50} values of less than 1μM (Figure 3). Six of the compounds which had been previously tested and confirmed[14] were reconfirmed here, but there were 18 compounds that were considered exoerythrocytic-stage active hits in the HCI assay and not in the luciferase-based assay. This is likely due to the higher initial screening concentrations used in the luciferase-based assay (50 μM compared to 10 μM in the HCI assay) leading to increased HepG2 cytotoxicity, as all of these compounds inhibited Pb-Luc activity but were toxic at 50 μM. It should be noted that due to the sensitivity of the luciferase assay and to minimize cytotoxicity, we advise starting with lower initial screening concentrations for future high-throughput screening.

Screening the Broad Diversity-Oriented Synthesis library

To assess performance in an unbiased screening library, two sets of Diversity-Oriented Synthesis (DOS) derived compounds were screened (outlined in Figure S3). These diverse compounds combine the stereochemical and skeletal complexity of the entire ensemble of natural products and the efficiency of high-throughput synthesis [22, 23]. This is an attractive validation library because multiple stereoisomers of each structural type are included, which permits a unique type of structure–activity relationship measurements. The first set included 9,886 compounds selected to represent the structural diversity of the scaffolds from the Broad Institute's 100,000 DOS compound library. This 'informer set' was tested as a naïve library with respect to activity against *Plasmodium*. The second set comprised 89 compounds previously shown to be active in a *P. falciparum* erythrocytic-stage assay (IC_{50} <

2 μM, Nobutaka Kato et al., unpublished results). Compounds that inhibited the luciferase signal >75% were scored as hits. From the informer set (hit rate = 0.6%), 60 hits and 4 inconclusive (only active in one replicate) were identified and 12 hits were identified from the erythrocytic-stage active set (hit rate = 13.4%). All available compounds (58) plus 25 additional weak actives (60–74% inhibition) from the informer set were tested in dose response in the primary exoerythrocytic-stage assay and also in a SYBR Green erythrocytic-stage assay[24]. All of the compounds from the erythrocytic-stage active set retested at dose with an IC_{50} < 5 μM and 10 of these compounds had an IC_{50} < 1 μM. In all, 72% (60 compounds) of the naïve informer set hits retested with IC_{50}s < 5 μM. A third of these had an IC_{50} < 1 μM (see Additional File 2 for full screening results). Finally, stereoisomers for selected hits were also examined in dose response. These data (Figure 4A) showed stereoselective inhibition; for example, only the S,S,S stereoisomer, BRD0326, is active (IC_{50} = 0.152 μM) in a set of eight stereoisomers tested.

MMV Malaria Box and Broad Library exoerythrocytic-stage active chemical clustering identifies active scaffolds and important targets

To cross validate these data, we first identified scaffolds that were enriched for compounds with exoerythrocytic-stage activity (relative to erythrocytic-stage or no antimalarial activity) using compound clustering. Given the small size of our initial compound set, we combined the MMV Malaria Box compounds with a GNF library consisting of 4,422 compounds that were previously screened for exoerythrocytic-stage activity in *P. berghei*[14]. Merging the libraries allowed us to determine if there was any overlap in scaffold hits between the two compound sets. The 4,822 compounds were clustered using a hierarchical clustering method based on substructure similarity. To define scaffold groups, we separated clusters based on a minimum Tanimoto coefficient requirement of 0.65, resulting in 2,335 total clusters that ranged in size from 1–45 compounds. DOS library compounds were also included, but given that the library was designed to eliminate structural redundancy, it was expected that DOS compounds would not contribute significantly to any scaffold clusters.

We identified 15 scaffold series that showed specific enrichment in exoerythrocytic-stage activity with rates higher than expected by chance ($p < 0.001$) (Figure 5). The scaffold clustering showed multiple scaffold families already known to be active. One is the diaminotriazine scaffold (1228) similar to the diaminopyrimidine found in antifolate drugs such as pyrimethamine (probability of enrichment by chance = 4.29e-7). Another is a tetracyclic benzothiazepine scaffold, cluster 1096, that has shown to target the Q_0 site of cytochrome bc1[25]. Several enriched quinolone compounds (GNF-Pf-2549, GNF-Pf-4577, GNF-Pf-5037; cluster 342) were similar to ELQ300, a possible Q_1 site cytochrome bc1 inhibitor[26] with known causal prophylactic activity in mouse models of malaria[27]. In addition, cluster 1096 may contain inhibitors of the electron transport chain (DHOD or cytochrome bc1) as do the three 4-quinolinol scaffolds (clusters 1122, 1613 and 2061). The compounds that were the precursors of the imidazolopiperazine compound in clinical trials, KAF156[28], were also found in a cluster of three compounds (GNF-Pf-5069, GNF-Pf-5179, GNF-Pf-5466; cluster 849). These compounds work by an unknown mechanism of action, but resistance is conferred by mutations in the *P. falciparum* cyclic amine resistance locus

(Pfcarl)[14]. Additionally, compounds in cluster 2045 have some structural similarity to *P. falciparum* histone methyltransferase inhibitors[29].

Although most of the over-represented scaffolds have been investigated as starting points of antimalarial drug discovery in recent years, there were also novel notable singleton molecules whose hepatic stage activity had not been previously described. For example, MMV666693 (the most potent compound from the exoerythrocytic-stage screen of the MMV Malaria Box) also strongly inhibits erythrocytic-stage *P. falciparum* with IC_{50} values reported below 100 nM (Table S1, Additional File 1). This compound was previously identified as an allosteric inhibitor of *P. falciparum* Kinesin-5, a microtubule cross-linking enzyme required for cell division[4]. It is therefore interesting to speculate that targeting this enzyme may be an efficient means to inhibit parasite replication across multiple developmental stages.

Compounds with exclusive activity against exoerythrocytic stages

Compounds that are active only against exoerythrocytic stages, but not erythrocytic stages, may represent new opportunities for development of drugs for which resistance acquisition may be less of a problem. While 42 of the 63 exoerythrocytic-stage DOS compounds were active in both the exoerythrocytic- and erythrocytic-stage assays, others could be starting points for such drugs. Several of the compounds that were identified in the DOS library unbiased screen are highlighted in Figure 4A. In particular, cyanoazetidine and a bicyclic azetidine series are shown. Although BRD7539 is active in both the exoerythrocytic- and asexual erythrocytic-stage assays, BRD9781 (its stereoisomer) is only active in the exoerythrocytic-stage assay. Although BRD7539 targets the *Plasmodium* DHODH enzyme[30], based on its profile across lifecycle stages, we suspect that BRD9781 has a different target. These results suggest the important role of stereochemistry in inhibiting different biological targets. BRD47390 appears to result in specific activity in the exoerythrocytic-stage assay, whereas the DOS Phenylalanine–tRNA ligase inhibitor is active against blood- and exoerythrocytic-stages. BRD0326, which has identical stereochemistry to BRD7539 but has differing functionality at the azetidine nitrogen, also has no erythrocytic-stage activity and may have yet another target. Further testing in a DHODH assay[31] confirmed that BRD0326 and BRD9781 are inactive (data not shown). BRD0326, BRD9781, and BRD47390 were all retested at dose along with all of their stereoisomers. With the exception of BRD7539, which targets DHODH, these compounds displayed stereoselective activity (Figure 4B). Overall these data show that up to a third of the hits in a screen of an unbiased library might have exclusive exoerythrocytic activity, targeting either unique EEF parasite targets or the host factors needed to support parasite replication.

Cross-validation using phenotypic assays to assess time of action during exoerythrocytic-stage development

We sought to further confirm exoerythrocytic-stage activity for the three most potent MMV Malaria Box hits by an orthogonal and complementary assay. This assay utilizes a previously described flow cytometry-based method[32, 33] to measure four specific metrics during exoerythrocytic-stage development: 1) sporozoite traversal, 2) sporozoite invasion, 3) EEF frequency, and 4) EEF development. The assay uses *P. berghei* expressing GFP (Pb-

GFP) infection of Huh7.5.1 cells, (Figure 6), a related exoerythrocytic cell line that can also be used to study EEF development (Figure S4) and measurements are taken at 2 and 48 hours post infection.

At 2 hours post infection, the number of hepatocytes that have been traversed and invaded is measured. Sporozoite traversal is inferred based on the observation that traversal temporarily ruptures the plasma membrane of hepatocytes, allowing high molecular weight rhodamine-dextran to stain cells that have been traversed but not invaded[34]. Sporozoite invasion is measured by the percentage of cells expressing GFP and not rhodamine-dextran, as the parasite enters the cells via a moving tight junction, excluding rhodamine-dextran[34]. Double positive cells, expressing both GFP and rhodamine-dextran, likely represent a population of non-productively infected cells, or cells in the process of being traversed by parasite, and are therefore not used in the measurements of traversal and invasion[33]. Cytochalasin D, a potent inhibitor of actin polymerization, is used as a positive control for traversal and invasion inhibition at 2 hours post infection as it has been previously demonstrated to reduce sporozoite motility (Figure 6A)[33].

At 48 hours post infection, the frequency and development (size) of exoerythrocytic-stage EEFs can be measured. The frequency of EEFs is determined by the percentage of cells expressing GFP at 48 hours post infection. KDU691, which inhibits *Plasmodium* phosphatidylinositol 4-kinase (PI(4)K), an enzyme that phosphorylates its phosphoinositide substrate to regulate intracellular signaling and trafficking [35], was used as a positive control because it was shown to significantly decrease the number of exoerythrocytic-stage EEFs (Figure 6A). At the same time, the assay measures EEF development by reporting GFP mean fluorescence intensity (MFI), an indicator of EEF size. Here, atovaquone serves as a positive control (Figure 6A).

As predicted, all compounds led to changes in cell populations that were detectable by flow cytometry (Figure 6B). At 48 hours post infection, all of the compounds tested led to a significant decrease in the EEF size, but not frequency, similar to that of atovaquone (Figure 6B). In addition, MMV666693 also appears to have a slight effect on sporozoite traversal of hepatocytes at 2 hours post infection (Figure 6B). Somewhat unexpectedly, sporozoite invasion at 2 hours post infection was not affected by MMV666693, and rather, slightly increased. Unlike KDU691, none of these compounds affected EEF frequency. While further investigation is needed to better understand the specific mode of action, these results suggest that these compounds are acting primarily during EEF development. An important caveat of the flow cytometry-based assay is that there may be prolonged fluorescence well after parasites have lost viability [36].

To provide further validation of EEF development inhibition, MMV666693, MMV007160, and MMV665916, were characterized in an exoerythrocytic-stage time of action assay and compared to compounds with known activity in hepatic stages. This included atovaquone, which targets mitochondrial cytochrome bc1 complex and therefore inhibits the parasite's electron transport chain during all developmental stages[5] (Figure 7B). Pyrimethamine inhibits dihydrofolate reductase (DHFR) and thus the synthesis of purines and pyrimidines required for DNA synthesis [37]. We also included several compounds in development such

as DDD107498, which inhibits *Plasmodium* translation elongation factor 2 (eEF2)[38], as well as KDU691[35]. A third compound, GNF179, whose target has not been elucidated but which has potent causal prophylactic activity in mice and resistance mediated by mutations in the aforementioned *Pf*carl gene, was also included[14]. Compounds were added in 12-point serial dilutions (10 μM to 56 pM) or washed out to be present during specific time frames throughout exoerythrocytic-stage development. Their activity was measured using a modified 384-well version of our high-throughput luciferase assay and bioluminescence recorded at 48 hours post-infection.

The assay supported the flow cytometry data and showed that MMV666693 and MMV007160 inhibit parasite replication during all time-points during exoerythrocytic-stage EEF development, and seem to be most potent when added during trophozoite development 6–24 hours post infection (Figure 7B). Unlike the other compounds tested, MMV665916 may need longer incubation *in vitro* in order to achieve optimal activity against exoerythrocytic-stage parasites, as all of the developmental time-points tested resulted in a more than 10-fold IC_{50} change compared to the 2–50 hours post infection control (Figure 7B). These data highlight how exoerythrocytic-active compounds may be further classified and how this assay may reveal information about a compound's mechanism of action.

Conclusions

The assays described here provide a high-throughput approach to identify scaffolds or scaffold families that will have causal prophylactic activity. Although our assay depends on rodent malaria parasites which are not infectious to humans, they have an advantage over human parasites because mosquitos infected with *P. berghei* or *P. yoelii* can be handled and shipped more easily. In addition, the number of sporozoites per mosquito is high (~20,000) enabling higher-throughput methods and evaluation of more starting points. This reduces cost (20 cents per well) as mosquito production and mosquito dissection are very labor intensive. One concern is that activity tests using rodent malaria parasites might not translate into activity against human parasites. In cases where a compound is also active against *P. falciparum* erythrocytic-stages, this is less likely to be a concern. In the small number of cases where compounds are not active in erythrocytic-stages, additional testing using exoerythrocytic-stages of *P. falciparum* or *P. vivax* may be warranted. Compounds of this class could be particularly interesting as leads for drugs that could be used in malaria elimination and eradication campaigns because they could be developed into drugs that could provide long-acting protection and which would not have the same resistance-development liabilities as compounds that act against the billions of erythrocytic-stage parasites that teem in an infected human. There is also the possibility that *P. falciparum*- or *P. vivax*-specific hits may be lost, however, this is likely a small number of compounds given the screening throughput capacity of the assay.

An unanswered question is whether leads identified with this assay will have radical cure activity. Primaquine and tafenoquine are the only two compounds that can provide radical cures and both behave poorly in cellular assays such as those described here because they depend on host organismal metabolism. These compounds are not even particularly active in assays that involve primary hepatocytes[39]. Likewise, we have recently tested a number of

MMV Malaria Box screening hits in an *ex vivo P. cynomolgi* model of hypnozoite development[40], however, only one compound, MMV007224, had moderate activity (at 10 μM) against small or large forms in the assay (Table S2). Interestingly, this was also the only compound of the set tested with any pharmacokinetic exposure *in vivo*[41]. This highlights the utility of using hepatoma cells rather than primary hepatocytes for screening purposes, as compounds with less than favorable pharmacokinetic properties can be evaluated for activity. As exoerythrocytic-stage active compounds identified in this report will also likely include inhibitors of *Plasmodium* exoerythrocytic-stage hypnozoites, it will be important to address compound metabolic stability *in vitro* and bioavailability *in vivo* during the development of novel hypnozoite models. This class of compounds will represent an important starting point for the development of novel treatments capable of providing a malaria radical cure.

Materials & Methods

Compound libraries

MMV Validation set of antimalarials—This collection of 50 known antimalarial powders were obtained from the MMV and are all commercially available and active primarily against erythrocytic-stage malaria parasites.

MMV Malaria Box—This open source compound library is comprised of 400 diverse open source compounds with proven antimalarial activity. 200 of these compounds are described by MMV as ‘drug-like’ and 200 as ‘probe-like’ compounds[18]. They have been distilled down from ~20,000 hits generated from a screening campaign of 4 million compounds from the libraries of St. Jude’s Children’s Hospital, Novartis, and GSK. All compounds are commercially available and the library is also available for free from MMV as long as the resulting data are published and placed in the public domain.

Broad Diversity-Oriented Synthesis Library—Two sets of compounds were tested from the Broad Diversity-Oriented Synthesis (DOS) library of 100,000 compounds. The first set included 9,886 compounds selected to represent the structural diversity of all of the scaffolds. This ‘informer’ set was used as a naïve library to screen for compounds with unknown activity against *Plasmodium*. The second set was comprised of 89 compounds previously shown to be active in a *P. falciparum* erythrocytic-stage assay (IC_{50} < 2 μM, Nobutaka Kato, unpublished results).

Parasites

P. berghei-ANKA-GFP-Luc-SM_{CON} (Pb-Luc)[42] and *P. berghei-GFP* (Pb-GFP)[35] sporozoites were obtained by dissection of infected *Anopheles stephensi* mosquito salivary glands. Dissected salivary glands were homogenized in a glass tissue grinder and filtered twice through nylon cell strainers (20 μm pore size, Millipore SCNY00020) and counted using a Neubauer hemocytometer. The sporozoites were kept on ice until needed. Both Pb-Luc and Pb-GFP infected *A. stephensi* mosquitoes were obtained from the Insectary Core Facility at New York University.

Cell lines

HepG2-A16-CD81^{EGFP}[20] cells stably transformed to express a GFP-CD81 fusion protein were cultured at 37 °C and 5% CO_2 in DMEM (Invitrogen, Carlsbad, USA) supplemented with 10% FCS, 0.29 mg/ml glutamine, 100 units penicillin and 100 μg/ml streptomycin. Huh7.5.1 cells were cultured at 37 °C and 5% CO_2 in DMEM (Invitrogen, Carlsbad, USA) supplemented with 10% FCS (Corning cat# 35-011-CV), 200 U/ml penicillin, 200 μg/ml streptomycin (Invitrogen cat# 15140-122), 10 mM Hepes (Invitrogen cat# 15630-080), 1× Glutamax (Invitrogen cat # 35050-061), 1x non-esential amino acids (Invitrogen). During infection, cell media was supplemented with 50μg/ml gentamycin and 50 μg/ml neomycin. After infection, the antimycotic 5-fluorocytosine at a final concentration of 50 μg/ml was added to the media.

High-content imaging

The high-content imaging experiments were performed as previously described[14]. Briefly, we used the HepG2-A16-CD81^{EGFP} host cells and either the *P. yoelii* or Pb-Luc rodent malaria parasites. We seeded the cells in 384-well plates and infected them with a ratio of 2:1 (cells:sporozoites). After staining the parasites with a polyclonal mouse anti-*Py*HSP70 antibody, these data were acquired (image analysis) with the Perkin Elmer Opera. Average parasite size per well served as the primary readout for compound effectiveness.

Luciferase-based high-throughput screening

Sporozoite infection—For the Pb-Luc high-throughput screen, we utilized *P. berghei* since its higher infection rates of immortal human hepatocyte cell lines are more conducive to high-throughput screening than the infection rates of human malaria parasites. *P. berghei* is able to infect human hepatocarcinoma HepG2 cells expressing the tetraspanin CD81 receptor[20]. 3×10^3. HepG2-A16-CD81^{EGFP} cells in 5 μl medium (2×10^5 cells/ml, 5% FBS, 5×x Pen/Strep/Glu) were seeded into 1536-well, white, solid-bottom plates (Ref# 789173-F, Greiner Bio-One) 20–26 hours prior to the actual infection. 18 hours prior to infection, 50 nl of compound in DMSO (0.5% final DMSO concentration per well) were transferred with a PinTool (GNF Systems) into the assay plates (10 μM final concentration). Atovaquone (12-point serial dilution starting at 10 μM) and 0.5% DMSO were used as positive and negative controls, respectively. Pb-Luc sporozoites were freshly dissected and their concentration adjusted to 200 sporozoites per μl. Penicillin and streptomycin were added at 5x concentration for a final 5x concentration in the well. The increased antibiotic concentration did not interfere with parasite or HepG2-A16-CD81^{EGFP} growth. The HepG2-A16-CD81^{EGFP} cells were then infected with 1×10^3 sporozoites per well (5 μl) using a single tip Bottle Valve liquid handler (GNF), and the plates were centrifuged for 3 minutes at room temperature and at 330× g (Eppendorf 5810 R centrifuge) on lowest acceleration and brake setting. The plates were then incubated at 37°C for 48 hours in 5% CO_2 with high humidity to minimize media evaporation and edge effect.

Bioluminescence quantification of exoerythrocytic forms (EEFs)—After incubation, the parasite EEF growth was quantified by bioluminescence measurement. Media was removed by spinning the inverted plates at 150× *g* for 30 seconds. 2 μl BrightGlo

reagent (Promega) were dispensed with the MicroFloliquid handler (BioTek). Immediately after addition of the luminescence reagent, the plates were vortexed at median intensity setting for 10 seconds and read by an EnVision Multilabel Plate Reader (PerkinElmer). IC_{50} values were obtained using measured bioluminescence intensity and a non-linear variable slope four parameter regression curve fitting model in Prism 6 (GraphPad Software Inc).

Bioluminescence quantification of HepG2 cytotoxicity—After incubation, the HepG2 cytotoxicity was assessed by removing the media through an inverted spin of the plates at 150× *g* for 30 seconds and addition of 2 μl CellTiterGlo reagent (Promega diluted 1:2 with deionized water) per well using the MicroFloliquid handler (BioTek). Immediately after addition of the luminescence reagent, the plates were vortexed for 10 seconds and read with an EnVision Multilabel Reader (PerkinElmer).

Bioluminescence quantification of compound luciferase inhibition—After a 3 hour incubation period, 2 μl BrightGlo (Promega) were added to the wells with the MicroFlo liquid handler (BioTek). Immediately after addition, the plates were read by an EnVision Multilabel Reader (PerkinElmer).

Bioinformatic analysis of EEF inhibition, HepG2 cytotoxicity and luciferase inhibition—For the first screening round, the luminescence reads from each 1536-well plate were analyzed separately. Briefly, a lack of inhibition was defined as the average DMSO readings (64 wells) minus the baseline inhibition readings. For both, the first and second round of screening, the baseline for the EEF inhibition was defined as the average of the five highest atovaquone concentrations (10 wells), the baseline for the HepG2 cytotoxicity was defined as the average of the highest puromycin concentrations (8 wells), and the baseline of the luciferase inhibition assay was defined as the average of 48 wells with 500 μM resveratrol. For the first round of screening, we determined the inhibition percentage relative to the normalized well concentrations for each compound. This analysis was repeated for every 1536-well plate. For the second reconfirmation round of screening, IC_{50} values were obtained using the average normalized bioluminescence intensity of 4 wells per concentration and plate (96 wells in total for each compound) and a nonlinear variable slope four parameter regression curve fitting model in Prism 6 (GraphPad Software Inc).

Culturing asexual erythrocytic-stage (AES) parasites

P. falciparum parasites were cultured in complete medium containing 5% hematocrit in a low-oxygen atmosphere composed of 1% oxygen, 3% carbon dioxide and 96% nitrogen at 37°C. Complete medium consists of RPMI medium 1640 (with L-glutamine, without phenol red, Thermo Fisher Scientific) supplemented with 4.3% heat-inactivated O^+ human serum, 0.2% AlbuMAX II lipid-rich BSA, 0.014 mg/ml hypoxanthine, 3.4 mM NaOH, 38.4 mM Hepes, 0.2% glucose, 0.2% sodium bicarbonate and 0.05 mg/ml gentamicin.

Asexual erythrocytic-stage screening in a 1536-well plate format

Pathogenic asexual erythrocytic-stage parasites were screened using a modified fluorescence-based proliferation assay described previously[10]. Briefly, *P. falciparum* 3D7

parasites were cultured until a parasitemia of 3–6% was reached. The level of erythrocytic-stage parasitemia was determined by microscopic inspection of Giemsa-stained blood smears for the presence of parasites. A parasite suspension with 0.3% parasitemia and 4% hematocrit was prepared in screening medium consisting of RPMI medium 1640 (with L-glutamine, without phenol red) supplemented with 0.4% AlbuMAX II lipid-rich BSA, 0.014 mg/ml hypoxanthine, 3.4 mM NaOH, 38.4 mM Hepes, 0.2% glucose, 0.2% sodium bicarbonate and 0.05 mg/ml gentamicin. The parasite culture was gassed with 1% oxygen, 3% carbon dioxide and 96% nitrogen and stored at 37°C until used. Next, 3 μl of screening medium were dispensed into 1,536-well, black, clear-bottom plates (Ref# 789092-F, Greiner Bio-One, Kremsmünster, Austria) using the MultiFlo™Microplate dispenser (BioTek Instruments, VT, USA). For determining the IC_{50} values, 50 nl of compounds dissolved in DMSO (12-point serial dilutions (1:3) starting at 10 mM) were transferred into the assay plates (62.5 μM final drug concentration, 0.625% final DMSO concentration) using the Biomek® FXP Laboratory Automation Workstation (Beckman Coulter, CA, USA) with a PinTool (V&P Scientific, CA, USA). Artemisinin and DMSO were included as background and baseline controls, respectively. Next, 5 μl of prepared parasite suspension were dispensed into the 1,536-well plates resulting in a final parasitemia of 0.3% and a final hematocrit concentration of 2.5% (MultiFlo™Microplate dispenser). The assay plates were transferred into Ziploc™ bags and gassed with a gas mixture of 1% oxygen, 3% carbon dioxide and 96% nitrogen. After a 72 hour incubation at 37°C, 2 μl of detection solution consisting of 10x SYBR Green I (Thermo Fisher Scientific) in lysis buffer (20 mMTris/HCl, 5 mM EDTA, 0.16% Saponin, 1.6% Triton X-100) were added to the plates (MultiFlo™Microplate dispenser) and incubated for 24 hours at room temperature in the dark. After 24 hours, fluorescence signals were measured at 530 nm with a 485 nm excitation from the bottom using the 2104 EnVision®Multilabel Reader (PerkinElmer, MA, USA). After subtracting the signal of the highest concentration of artemisinin (background) from all output values and normalizing the values to the average DMSO signal, the IC_{50} values were calculated by using a non-linear variable slope regression curve-fitting model in GraphPad Prism (GraphPad Software Inc.).

Computational compound clustering

To evaluate clustering of exoerythrocytic-stage hits and enrichment of compound groups, the 400 compound MMV set was co-clustered with a set of > 4,000 compounds that had previously been evaluated in a *P. yoelii* high-content imaging assay[14]. Briefly, SMILESL (simplified molecular-input line-entry system) strings were loaded into R, and the maximum common substructure Tanimoto coefficient (MCS-TC) was calculated using the fmcsR package[43]. The compounds were then subsequently hierarchically clustered with the hclust package, using the ward.D2 agglomeration method pair clusters. To create compound bins, the tree branches were separated at a maximum pair-wise distance of 0.4. Hypergeometric mean statistical tests were applied to each compound bin to identify sets where exoerythrocytic-stage activity was enriched.

Flow cytometry assay

Exoerythrocytic-stage Pb-GFP traversal, invasion, and schizont development were measured using a previously established flow cytometry-based method[33]. Briefly, 24 hours prior to

infection, 1.75×10^5 Huh7.5.1 cells were seeded in 24-well plates in 1 ml of DMEM hepatocyte culture medium for the traversal and invasion assay, as well as for the quantitation of EEF size and frequency. Pb-GFP sporozoites were freshly isolated from infected *Anopheles stephensi* mosquitoes as described above, and 3.5×10^4 or 7.0×10^4 sporozoites were added to the cells for the traversal/invasion assay or EEF quantitation assay, respectively, and incubated for 2 hours. Rhodamine-dextran was added to the wells at a final concentration of 1 mg/ml for the traversal and invasion assay. The cells were washed after the 2 hour infection, and assayed using flow cytometry for Rhodamine-dextran and GFP signal (traversal and invasion, respectively), or incubated for 48 hours and assayed by flow cytometry for GFP frequency and MFI (EEF frequency and size, respectively). Data were analyzed using the FlowJo Software.

Pb-Luc time of action assay

For the Pb-Luc time-course assay, we seeded 1×10^4 Huh7.5.1 cells in 30 μl hepatocyte culture media per well in a 384-well plate (Greiner Bio) 24 hours before infection. Pb-Luc sporozoites were freshly dissected from infected *Anopheles stephensi* mosquitos and 5×10^3 sporozoites in 30 μl were added to each well. The plates were centrifuged for 5 minutes at 330× *g* and incubated for 2 hours at 37°C and 5% CO_2. After incubation, media was removed and 50 μl fresh culture media was added. 12-point serial dilutions of compound in DMSO were added and removed from the plates at the indicated time-points post infection. At 48 hours post infection, media was removed from the plates and 20 μl BrightGlo Reagent (Promega) was added to each well. Luciferase light units were measured by bioluminescence using an EnVision Multilabel Plate Reader (PerkinElmer).

P. cynomolgi liver assay

The *P. cynomolgi* assay was performed as previously reported by Zeeman et. al.[40]. All Rhesus macaques (*Macaca mulatta*) used in this study were bred in captivity for research purposes, and were housed at the Biomedical Primate Research Centre (BPRC; AAALAC-certified institute) facilities under compliance with the Dutch law on animal experiments, European directive 2010/63/EU and with the ‘Standard for Humane Care and Use of Laboratory Animals by Foreign institutions’ identification number A5539-01, provided by the Department of Health and Human Services of the US National Institutes of Health. The local independent ethical committee first approved all protocols.

Supplementary Material

Refer to Web version on PubMed Central for supplementary material.

Acknowledgments

We thank our colleagues from The Genomics Institute of the Novartis Research Foundation, in particular Richard Glynne, Purvi Sanghvi, Annie Mak and Jason Matzen. They provided insight, expertise, and assistance that greatly assisted the research.

The mosquitoes were supplied by the Insectary Core Facility at New York University School of Medicine (http://microbiology-parasitology.med.nyu.edu/research/parasitology/insectary-core-facility-and-parasite-culture). Infection of mosquitoes was performed by bite of mice infected with the same parasite in blood stage. This procedure was carried out in strict accordance with the recommendations in the Guide for the Care and Use of

Laboratory Animals of the National Institutes of Health. The protocol was approved by the Institutional Animal Care and Use Committee of New York University School of Medicine (Protocol Number 150816), which is fully accredited by the Association For Assessment and Accreditation Of Laboratory Animal Care International (AAALAC).

The authors acknowledge the Medicines for Malaria Venture (MMV) for access to the MMV Malaria Box. SM, JS, CR, and YA was supported by MMV. VC was supported by the Bill and Melinda Gates Foundation (OPP104040). EAW was funded by the Bill and Melinda Gates Foundation (OPP1054480), MMV, and NIH (R01AI090141 and R01AI103058). MM was supported by the National Science Foundation (NSF) GRPF (DGE1144152), NK, EC, CS and SLS was supported by the Bill and Melinda Gates Foundation (OPP1032518). SLS is an investigator at the Howard Hughes Medical Institute. CM, KG, and MI were funded by the Welcome Trust (WT078285). AMZ and CHMK were funded by the Wellcome Trust (WT078285) and received additional funding from MMV. The authors would like to acknowledge Omar Vandal for assistance with grant management, and Paula Maguina for administrative assistance.

References

1. Carter R, Mendis KN. Evolutionary and historical aspects of the burden of malaria. Clinical microbiology reviews. 2002; 15:564–594. [PubMed: 12364370]
2. Snow RW, Guerra CA, Noor AM, Myint HY, Hay SI. The global distribution of clinical episodes of Plasmodium falciparum malaria. Nature. 2005; 434:214–217. [PubMed: 15759000]
3. Sachs J, Malaney P. The economic and social burden of malaria. Nature. 2002; 415:680–685. [PubMed: 11832956]
4. Sinka ME, Bangs MJ, Manguin S, Rubio-Palis Y, Chareonviriyaphap T, Coetzee M, Mbogo CM, Hemingway J, Patil AP, Temperley WH, Gething PW, Kabaria CW, Burkot TR, Harbach RE, Hay SI. A global map of dominant malaria vectors. Parasites & vectors. 2012; 5:69. [PubMed: 22475528]
5. Flannery EL, Chatterjee AK, Winzeler EA. Antimalarial drug discovery - approaches and progress towards new medicines, Nature reviews. Microbiology. 2013; 11:849–862. [PubMed: 24217412]
6. Prudencio M, Rodriguez A, Mota MM. The silent path to thousands of merozoites: the Plasmodium liver stage, Nature reviews. Microbiology. 2006; 4:849–856. [PubMed: 17041632]
7. Wells TN, Burrows JN, Baird JK. Targeting the hypnozoite reservoir of Plasmodium vivax: the hidden obstacle to malaria elimination. Trends in parasitology. 2010; 26:145–151. [PubMed: 20133198]
8. Clark IA, al Yaman FM, Jacobson LS. The biological basis of malarial disease. International journal for parasitology. 1997; 27:1237–1249. [PubMed: 9394194]
9. Baker DA. Malaria gametocytogenesis. Molecular and biochemical parasitology. 2010; 172:57–65. [PubMed: 20381542]
10. Delves M, Plouffe D, Scheurer C, Meister S, Wittlin S, Winzeler EA, Sinden RE, Leroy D. The activities of current antimalarial drugs on the life cycle stages of Plasmodium: a comparative study with human and rodent parasites. PLoS medicine. 2012; 9:e1001169. [PubMed: 22363211]
11. Tan KR, Magill AJ, Parise ME, Arguin PM. Doxycycline for malaria chemoprophylaxis and treatment: report from the CDC expert meeting on malaria chemoprophylaxis. The American journal of tropical medicine and hygiene. 2011; 84:517–531. [PubMed: 21460003]
12. Hyde JE. Mechanisms of resistance of Plasmodium falciparum to antimalarial drugs. Microbes and infection / Institut Pasteur. 2002; 4:165–174. [PubMed: 11880048]
13. Ganesan S, Chaurasiya ND, Sahu R, Walker LA, Tekwani BL. Understanding the mechanisms for metabolism-linked hemolytic toxicity of primaquine against glucose 6-phosphate dehydrogenase deficient human erythrocytes: evaluation of eryptotic pathway. Toxicology. 2012; 294:54–60. [PubMed: 22330256]
14. Meister S, Plouffe DM, Kuhen KL, Bonamy GM, Wu T, Barnes SW, Bopp SE, Borboa R, Bright AT, Che J, Cohen S, Dharia NV, Gagaring K, Gettayacamin M, Gordon P, Groessl T, Kato N, Lee MC, McNamara CW, Fidock DA, Nagle A, Nam TG, Richmond W, Roland J, Rottmann M, Zhou B, Froissard P, Glynne RJ, Mazier D, Sattabongkot J, Schultz PG, Tuntland T, Walker JR, Zhou Y, Chatterjee A, Diagana TT, Winzeler EA. Imaging of Plasmodium liver stages to drive next-generation antimalarial drug discovery. Science. 2011; 334:1372–1377. [PubMed: 22096101]

15. Derbyshire ER, Mota MM, Clardy J. The next opportunity in anti-malaria drug discovery: the liver stage. PLoS pathogens. 2011; 7:e1002178. [PubMed: 21966266]
16. Reader J, Botha M, Theron A, Lauterbach SB, Rossouw C, Engelbrecht D, Wepener M, Smit A, Leroy D, Mancama D, Coetzer TL, Birkholtz LM. Nowhere to hide: interrogating different metabolic parameters of Plasmodium falciparum gametocytes in a transmission blocking drug discovery pipeline towards malaria elimination. Malaria journal. 2015; 14:213. [PubMed: 25994518]
17. Derbyshire ER, Prudencio M, Mota MM, Clardy J. Liver-stage malaria parasites vulnerable to diverse chemical scaffolds. Proc Natl Acad Sci U S A. 2012; 109:8511–8516. [PubMed: 22586124]
18. Spangenberg T, Burrows JN, Kowalczyk P, McDonald S, Wells TN, Willis P. The open access malaria box: a drug discovery catalyst for neglected diseases. PloS one. 2013; 8:e62906. [PubMed: 23798988]
19. Janse CJ, Franke-Fayard B, Mair GR, Ramesar J, Thiel C, Engelmann S, Matuschewski K, van Gemert GJ, Sauerwein RW, Waters AP. High efficiency transfection of Plasmodium berghei facilitates novel selection procedures. Molecular and biochemical parasitology. 2006; 145:60–70. [PubMed: 16242190]
20. Silvie O, Greco C, Franetich JF, Dubart-Kupperschmitt A, Hannoun L, van Gemert GJ, Sauerwein RW, Levy S, Boucheix C, Rubinstein E, Mazier D. Expression of human CD81 differently affects host cell susceptibility to malaria sporozoites depending on the Plasmodium species. Cellular microbiology. 2006; 8:1134–1146. [PubMed: 16819966]
21. Ignowski JM, Schaffer DV. Kinetic analysis and modeling of firefly luciferase as a quantitative reporter gene in live mammalian cells. Biotechnology and bioengineering. 2004; 86:827–834. [PubMed: 15162459]
22. Dandapani S, Marcaurelle LA. Grand challenge commentary: Accessing new chemical space for ‘undruggable’ targets. Nature chemical biology. 2010; 6:861–863. [PubMed: 21079589]
23. Nielsen TE, Schreiber SL. Towards the optimal screening collection: a synthesis strategy. Angewandte Chemie (International ed. in English). 2008; 47:48–56. [PubMed: 18080276]
24. Plouffe D, Brinker A, McNamara C, Henson K, Kato N, Kuhen K, Nagle A, Adrian F, Matzen JT, Anderson P, Nam TG, Gray NS, Chatterjee A, Janes J, Yan SF, Trager R, Caldwell JS, Schultz PG, Zhou Y, Winzeler EA. In silico activity profiling reveals the mechanism of action of antimalarials discovered in a high-throughput screen. Proceedings of the National Academy of Sciences of the United States of America. 2008; 105:9059–9064. [PubMed: 18579783]
25. Dong CK, Urgaonkar S, Cortese JF, Gamo FJ, Garcia-Bustos JF, Lafuente MJ, Patel V, Ross L, Coleman BI, Derbyshire ER, Clish CB, Serrano AE, Cromwell M, Barker RH Jr, Dvorin JD, Duraisingh MT, Wirth DF, Clardy J, Mazitschek R. Identification and validation of tetracyclic benzothiazepines as Plasmodium falciparum cytochrome bc1 inhibitors. Chem Biol. 2011; 18:1602–1610. [PubMed: 22195562]
26. Capper MJ, O’Neill PM, Fisher N, Strange RW, Moss D, Ward SA, Berry NG, Lawrenson AS, Hasnain SS, Biagini GA, Antonyuk SV. Antimalarial 4(1H)-pyridones bind to the Qi site of cytochrome bc1. Proceedings of the National Academy of Sciences. 2015; 112:755–760.
27. Nilsen A, LaCrue AN, White KL, Forquer IP, Cross RM, Marfurt J, Mather MW, Delves MJ, Shackleford DM, Saenz FE, Morrisey JM, Steuten J, Mutka T, Li Y, Wirjanata G, Ryan E, Duffy S, Kelly JX, Sebayang BF, Zeeman AM, Noviyanti R, Sinden RE, Kocken CH, Price RN, Avery VM, Angulo-Barturen I, Jimenez-Diaz MB, Ferrer S, Herreros E, Sanz LM, Gamo FJ, Bathurst I, Burrows JN, Siegl P, Guy RK, Winter RW, Vaidya AB, Charman SA, Kyle DE, Manetsch R, Riscoe MK. Quinolone-3-diarylethers: a new class of antimalarial drug. Science translational medicine. 2013; 5:177ra137.
28. Kuhen KL, Chatterjee AK, Rottmann M, Gagaring K, Borboa R, Buenviaje J, Chen Z, Francek C, Wu T, Nagle A, Barnes SW, Plouffe D, Lee MC, Fidock DA, Graumans W, van de Vegte-Bolmer M, van Gemert GJ, Wirjanata G, Sebayang B, Marfurt J, Russell B, Suwanarusk R, Price RN, Nosten F, Tungtaeng A, Gettayacamin M, Sattabongkot J, Taylor J, Walker JR, Tully D, Patra KP, Flannery EL, Vinetz JM, Renia L, Sauerwein RW, Winzeler EA, Glynne RJ, Diagana TT. KAF156 is an antimalarial clinical candidate with potential for use in prophylaxis, treatment, and prevention

of disease transmission. Antimicrobial agents and chemotherapy. 2014; 58:5060–5067. [PubMed: 24913172]

29. Malmquist NA, Moss TA, Mecheri S, Scherf A, Fuchter MJ. Small-molecule histone methyltransferase inhibitors display rapid antimalarial activity against all blood stage forms in Plasmodium falciparum. Proceedings of the National Academy of Sciences of the United States of America. 2012; 109:16708–16713. [PubMed: 23011794]
30. Nobutaka Kato EC, Sakata-Kato Tomoyo, Maetani Micah, Bastien Jessica, Victoria Corey DC, Derbyshire Emily R, Dornan Gillian, Duffy Sandra, Eckley Sean, Koolen Karin MJ, TAL, Lukens Amanda K, Lund Emily, Riera Sandra, Bennett C, Meier JM, Mitasev Branko, Moss Eli L, Sayes Morgane, VanGessel Yvonne, Wawer Mathias J, Yoshinaga Takashi, Zeeman Anne-Marie, Avery Vicky M, Bhatia Sangeeta N, Burke John E, Catteruccia Flaminia, Clardy Jon C, Clemons Paul A, Dechering Koen J, Duvall Jeremy R, Foley Michael A, Gusovsky Fabian, Kocken Clemens HM, Morningstar Marshall L, Munoz Benito, Neafsey Daniel E, Winzeler Elizabeth A, Wirth Dyann F, Scherer Christina A, Schreiber Stuart L. Diversity synthesis yields multistage antimalarial inhibitors including of a novel target that results in low single-dose cures in mice. (In review).
31. Ross LS, Gamo FJ, Lafuente-Monasterio MJ, Singh OM, Rowland P, Wiegand RC, Wirth DF. In vitro resistance selections for Plasmodium falciparum dihydroorotate dehydrogenase inhibitors give mutants with multiple point mutations in the drug-binding site and altered growth. The Journal of biological chemistry. 2014; 289:17980–17995. [PubMed: 24782313]
32. Prudencio M, Rodrigues CD, Ataide R, Mota MM. Dissecting in vitro host cell infection by Plasmodium sporozoites using flow cytometry. Cellular microbiology. 2008; 10:218–224. [PubMed: 17697130]
33. Sinnis P, De La Vega P, Coppi A, Krzych U, Mota MM. Quantification of sporozoite invasion, migration, and development by microscopy and flow cytometry. Methods in molecular biology. 2013; 923:385–400. [PubMed: 22990793]
34. Mota MM, Pradel G, Vanderberg JP, Hafalla JC, Frevert U, Nussenzweig RS, Nussenzweig V, Rodriguez A. Migration of Plasmodium sporozoites through cells before infection. Science. 2001; 291:141–144. [PubMed: 11141568]
35. McNamara CW, Lee MC, Lim CS, Lim SH, Roland J, Nagle A, Simon O, Yeung BK, Chatterjee AK, McCormack SL, Manary MJ, Zeeman AM, Dechering KJ, Kumar TR, Henrich PP, Gagaring K, Ibanez M, Kato N, Kuhen KL, Fischli C, Rottmann M, Plouffe DM, Bursulaya B, Meister S, Rameh L, Trappe J, Haasen D, Timmerman M, Sauerwein RW, Suwanarusk R, Russell B, Renia L, Nosten F, Tully DC, Kocken CH, Glynne RJ, Bodenreider C, Fidock DA, Diagana TT, Winzeler EA. Targeting Plasmodium PI(4)K to eliminate malaria. Nature. 2013; 504:248–253. [PubMed: 24284631]
36. Corish P, Tyler-Smith C. Attenuation of green fluorescent protein half-life in mammalian cells. Protein engineering. 1999; 12:1035–1040. [PubMed: 10611396]
37. Peterson DS, Walliker D, Wellems TE. Evidence that a point mutation in dihydrofolate reductase-thymidylate synthase confers resistance to pyrimethamine in falciparum malaria. Proceedings of the National Academy of Sciences of the United States of America. 1988; 85:9114–9118. [PubMed: 2904149]
38. Baragana B, Hallyburton I, Lee MC, Norcross NR, Grimaldi R, Otto TD, Proto WR, Blagborough AM, Meister S, Wirjanata G, Ruecker A, Upton LM, Abraham TS, Almeida MJ, Pradhan A, Porzelle A, Martinez MS, Bolscher JM, Woodland A, Norval S, Zuccotto F, Thomas J, Simeons F, Stojanovski L, Osuna-Cabello M, Brock PM, Churcher TS, Sala KA, Zakutansky SE, Jimenez-Diaz MB, Sanz LM, Riley J, Basak R, Campbell M, Avery VM, Sauerwein RW, Dechering KJ, Noviyanti R, Campo B, Frearson JA, Angulo-Barturen I, Ferrer-Bazaga S, Gamo FJ, Wyatt PG, Leroy D, Siegl P, Delves MJ, Kyle DE, Wittlin S, Marfurt J, Price RN, Sinden RE, Winzeler EA, Charman SA, Bebrevska L, Gray DW, Campbell S, Fairlamb AH, Willis PA, Rayner JC, Fidock DA, Read KD, Gilbert IH. A novel multiple-stage antimalarial agent that inhibits protein synthesis. Nature. 2015; 522:315–320. [PubMed: 26085270]
39. Dembele L, Gego A, Zeeman AM, Franetich JF, Silvie O, Rametti A, Le Grand R, Dereuddre-Bosquet N, Sauerwein R, van Gemert GJ, Vaillant JC, Thomas AW, Snounou G, Kocken CH, Mazier D. Towards an in vitro model of Plasmodium hypnozoites suitable for drug discovery. PLoS ONE. 2011; 6:e18162. [PubMed: 21483865]

40. Zeeman AM, van Amsterdam SM, McNamara CW, Voorberg-van der Wel A, Klooster EJ, van den Berg A, Remarque EJ, Plouffe DM, van Gemert GJ, Luty A, Sauerwein R, Gagaring K, Borboa R, Chen Z, Kuhen K, Glynne RJ, Chatterjee AK, Nagle A, Roland J, Winzeler EA, Leroy D, Campo B, Diagana TT, Yeung BK, Thomas AW, Kocken CH. KAI407, a potent non-8-aminoquinoline compound that kills Plasmodium cynomolgi early dormant liver stage parasites in vitro. Antimicrobial agents and chemotherapy. 2014; 58:1586–1595. [PubMed: 24366744]

41. Van Voorhis, Wesley C.; JHA; Adelfio, Roberto; Ahyong, Vida; Akabas, Myles H.; Alano, Pietro; Alday, Aintzane; Resto, Yesmalie Alemán; Alsibaee, Aishah; Alzualde, Ainhoa; Andrews, Katherine T.; Avery, Simon V.; Avery, Vicky M.; Ayong, Lawrence; Baker, Mark; Baker, Stephen; Mamoum, Choukri Ben; Bhatia, Sangeeta; Bickle, Quentin; Bounaadja, Lotfi; Bowling, Tana; Bosch, Jürgen; Boucher, Lauren E.; Boyom, Fabrice F.; Brea, Jose; Brennan, Marian; Burton, Audrey; Caffrey, Conor R.; Camarda, Grazia; Carrasquilla, Manuela; Carter, Dee; Cassera, Maria Belen; Cheng, Ken Chih-Chien; Chindaudomsate, Worathad; Chubb, Anthony; Colon, Beatrice L.; Colón-López, Daisy C.; Corbett, Yolanda; Crowther, Gregory J.; Cowan, Noemi; D'Alessandro, Sarah; Dang, Na Le; Delves, Michael; DeRisi, Joseph L.; DeRisi, Joseph L.; Du, Alan Y.; Duffy, Sandra; El-Sayed, Shimaa Abd El-Salam; Ferdig, Michael T.; Fernández Robledo, José A.; Fidock, David A.; Florent, Isabelle; Fokou, Patrick VT.; Galstian, Ani; Gamo, Francisco Javier; Gokool, Suzanne; Gold, Ben; Golub, Todd; Gokool, Suzanne; Goldgof, Gregory M.; Guha, Rajarshi; Armand Guiguemde, W.; Gural, Nil; Kiplin Guy, R.; Hansen, Michael; Hanson, Kirsten K.; Hemphill, Andrew; van Huijsduijnen, Rob Hooft; Horii, Takaaki; Horrocks, Paul; Hughes, Tyler B.; Huston, Christopher; Igarashi, Ikuo; Ingram-Sieber, Katrin; Itoe, Maurice A.; Jadhav, Ajit; Jensen, Amornrat Naranuntarat; Jensen, Laran T.; Jiang, Rays HY.; Kaiser, Annette; Keiser, Jennifer; Ketas, Thomas; Kicka, Sebastien; Kim, Sunyoung; Kirk, Kiaran; Kumar, Vidya; Kyle, Dennis E.; Lafuente, Maria Jose; Landfear, Scott; Lee, Nathan; Lee, Sukjun; Lehane, Adele; Li, Fengwu; Little, David; Liu, Liqiong; Llinás, Manuel; Loza, Maria I.; Lubar, Aristea; Lucantoni, Leonardo; Lucet, Isabelle; Maes, Louis; Mansour, Nuha R.; March, Sandra; McGowan, Sheena; Vera, Iset Medina; Meister, Stephan; Mercer, Luke; Mestres, Jordi; Mfopa, Alvine N.; Misra, Raj N.; AB; Moon, Seunghyun; Moore, John P.; Müller, Joachim; Muriana, Arantza; Stephen Nakazawa Hewitt, MS.; Nare, Bakela; Nathan, Carl; Narraidoo, Nathalie; Nawaratna, Sujeevi; Ojo, Kayode K.; Ortiz, Diana; Panic, Gordana; Papadatos, George; Parapini, Silvia; Patra, Kailash; Pham, Ngoc; Prats, Sarah; Plouffe, David M.; Poulsen, Sally-Ann; Pradhan, Anupam; Quevedo, Celia; Quinn, Ronald J.; Rice, Christopher A.; Rizk, Mohamed Abdo; Ruecker, Andrea; St Onge, Robert; Samra, Jasmeet; Sanders, Natalie G.; Schlecht, Ulrich; Schmitt, Marjorie; Sinden, Robert; Silvestrini, Francesco; Smith, Dennis A.; Soldati, Thierry; Spitzmüller, Andreas; Stamm, Serge Maximilian; Sullivan, David J.; Sullivan, William; Suresh, Sundari; Suzuki, Brian M.; Suzuki, Yo; Joshua Swamidass, S.; Taramelli, Donatella; Tchokouaha, Lauve RY.; Thomas, David; Tonissen, Kathryn F.; Townson, Simon; Tripathi, Abhai K.; Trofimov, Valentin; Udenze, Kenneth O.; Ullah, Imran; Vallieres, Cindy; Vigil, Edgar; Vinetz, Joseph M.; Vinh, Phat Voong; Vu, Hoan; Watanabe, Naoaki; Weatherby, Kate; White, Pamela M.; Winzeler, Elizabeth A.; Wojcik, Edward; Wree, Melanie; Wu, Wesley; Yokoyama, Naoaki; Zollo, Paul HA.; Abla, Nada; Blasco, Benjamin; Burrows, Jeremy; Laleu, Benoît; Leroy, Didier; Spangenberg, Thomas; Wells, Timothy; Willis, Paul. Open-source drug discovery with the Malaria Box compound collection for neglected diseases and beyond. 2016 (In review).

42. da Cruz FP, Martin C, Buchholz K, Lafuente-Monasterio MJ, Rodrigues T, Sonnichsen B, Moreira R, Gamo FJ, Marti M, Mota MM, Hannus M, Prudencio M. Drug screen targeted at Plasmodium liver stages identifies a potent multistage antimalarial drug. The Journal of infectious diseases. 2012; 205:1278–1286. [PubMed: 22396598]

43. Srivastava IK, Morrisey JM, Darrouzet E, Daldal F, Vaidya AB. Resistance mutations reveal the atovaquone-binding domain of cytochrome b in malaria parasites. Molecular microbiology. 1999; 33:704–711. [PubMed: 10447880]

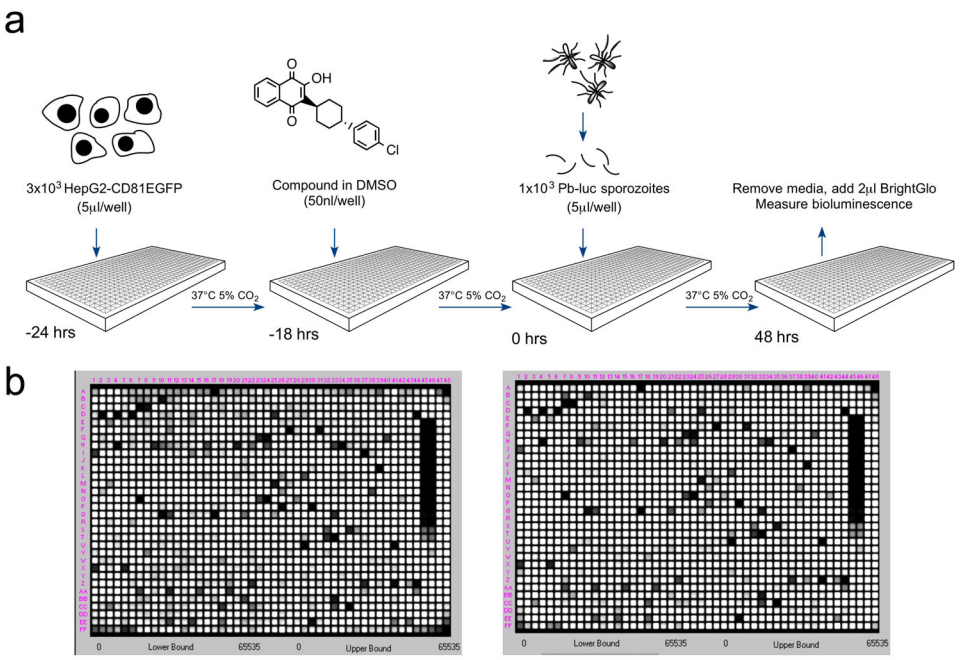

Figure 1. A luciferase-based high-throughput screening assay to identify malaria exoerythrocytic-stage inhibitors

a) Assay workflow. 24 hours prior to infection, 3×10^3 HepG2-A16-CD81^{EGFP} cells in 5 µl media were added to wells in a 1536-well assay plate. One to four hours later, 50 nl of compound dissolved in DMSO were added to the wells. At the time of infection, Pb-Luc sporozoites were freshly prepared from infected *A. stephensi* mosquitoes and diluted to a concentration of 1×10^3 in 5 µl media per well. After 48 hours, Pb-Luc growth within hepatocytes was measured by bioluminescence.

b) As a proof of concept, we screened two plates containing 2,816 natural compounds (GNF) in replicate. One set of replicates is shown here. The average Z factor for these plates was 0.82.

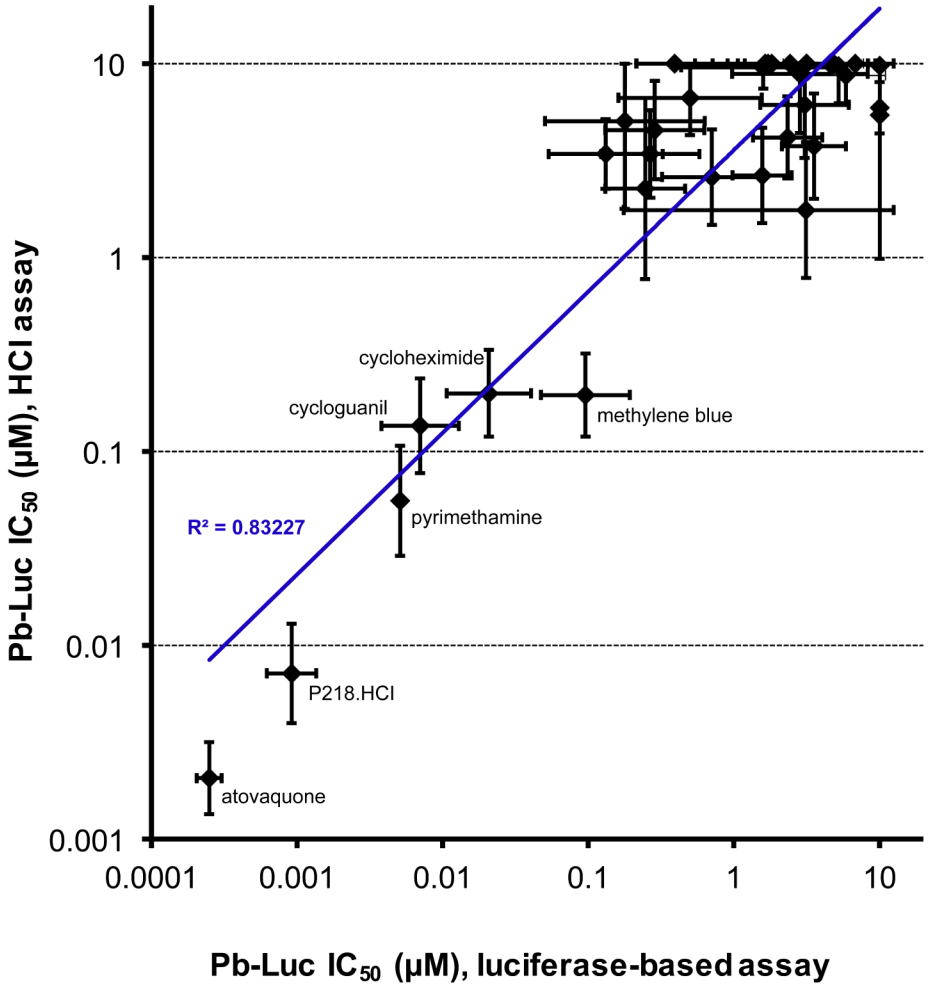

Figure 2. 1536-well luciferase-based screening assay is higher-throughput and more sensitive than former 384-well HCI assay

Pb-Luc IC_{50} values for the MMV validation set of antimalarials screened by the luciferase-based 1536-well assay and by the 384-well high-content imaging (HCI) assay are compared. Each data point represents a single antimalarial compound. The most active compounds in both assays are labeled. The assays generate Pb-Luc IC_{50} values that correlate very well with eachother, as demonstrated by an R^2 value of 0.83, however, the luciferase-based assay resulted in IC_{50}s roughly 10× lower than in the HCI assay.

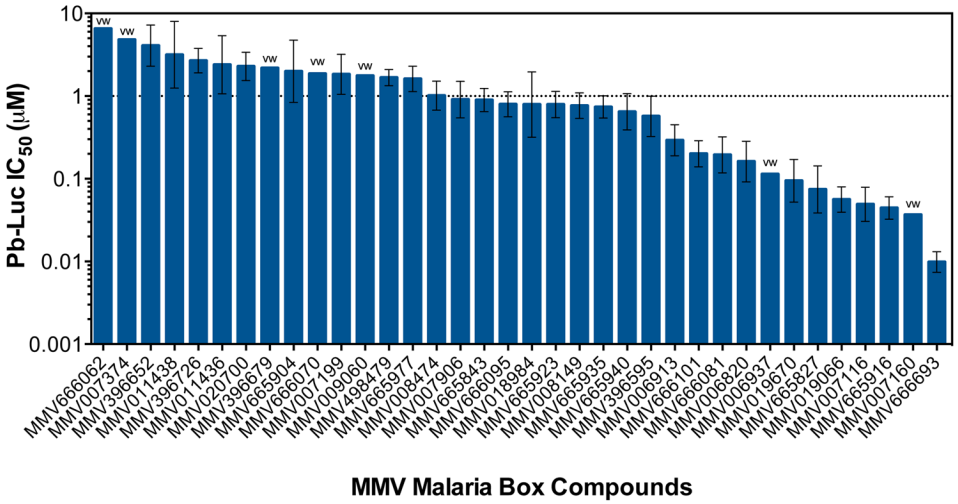

Figure 3. MMV Malaria Box compounds are identified as potent malaria exoerythrocytic-stage inhibitors

The 36 exoerythrocytic-stage active MMV Malaria Box hits with a Pb-Luc IC_{50} of less than 10 μM are shown with their respective IC_{50} values. Hits were also selected to demonstrate a HepG2 IC_{50} and a Luc IC_{50} of more than 10 μM. A line at 1 μM highlights that almost half of the exoerythrocytic-stage active hits display nanomolar potency. Error bars represent the 95% confidence interval.

a

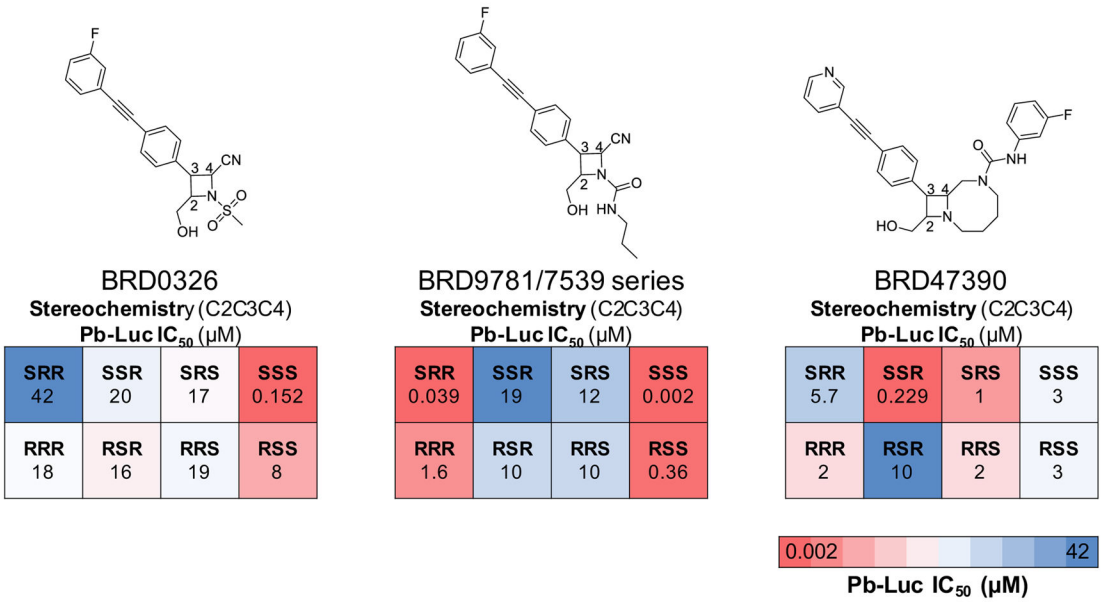

b

	BRD0326	BRD9781	BRD7539	BRD47390
Stereochemistry ($C_2C_3C_4$)	SSS	SRR	SSS	SSR
Exoeyrthrocytic-stage Pb-Luc IC_{50} (μM)	0.3 (0.15)	0.08 (0.04)	0.01 (0.002)	0.36 (0.23)
Erythrocytic-stage (Pf Dd2) IC_{50} (μM)	> 10	8.547	0.01	2.58
HepG2 cells CC_{50} (μM)	> 10	>10	> 10	> 10

Figure 4. DOS compounds exhibit stereoselective inhibition of Pb-Luc exoerythrocytic-stage parasite growth

a) Representative compounds and activity profiles with activity against *P. berghei* in HepG2 cells. Stereocenters (C_n) are listed below the corresponding chemical structure. Pb-Luc exoerythrocytic-stage activity was measured for each of the 8 possible stereoisomers (SRR, SSR, SRS, SSS, RRR, RSR, RRS, and RSS) of each compound. Three of the eight possible stereoisomers of BRD9781 have exoerythrocytic-stage activity, two with potent activity (SRR and SSS, IC_{50} <0.1 μM), and another with moderate activity (RSS, IC_{50} < 1 μM). B. One stereoisomer of BRD0326 (SSS) is active (IC_{50} < 1μM). C. Two stereoisomers of BRD47390 have significant exoerythrocytic-stage activity (SSR, IC_{50} < 0.1 μM; SRS, IC_{50} < 0.1 μM).

b) Compounds were tested in dose in the *P. berghei*/HepG2 assay, a Dd2 erythrocytic stage assay, and in a mammalian cell cytotoxicity assay. Compounds from three scaffold libraries are shown. Compounds were tested twice in the exoerythrocytic-stage assay; values from the second assay are shown in parentheses.

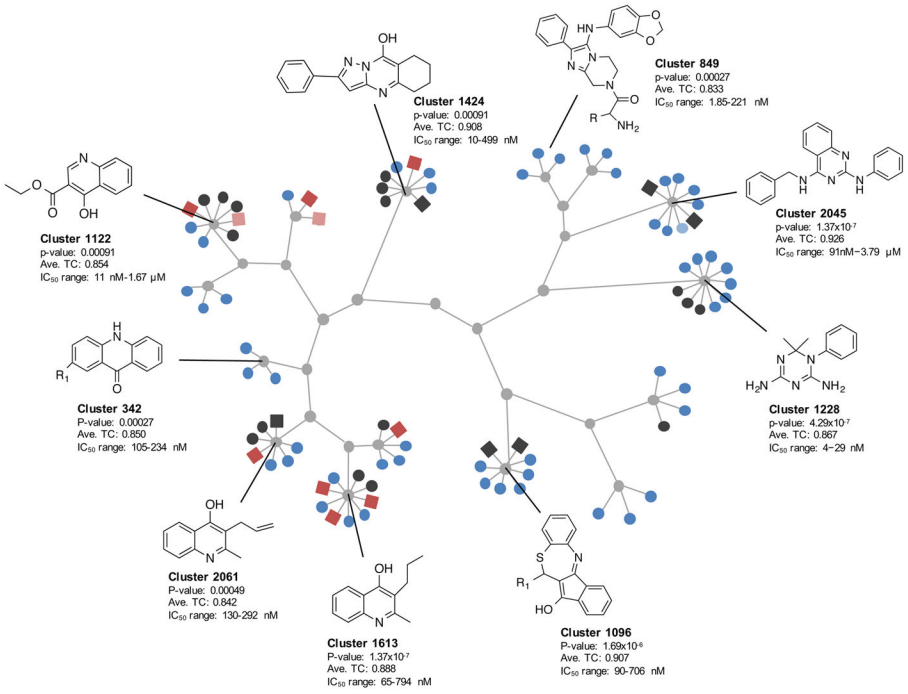

Figure 5. Exoerythrocytic-stage active MMV compounds display unique chemical scaffold clustering

Compounds of the GNF and MMV Malaria Box were clustered by their substructure similarity, binning sets based on main common substructure (Tanimoto average compound similarity ≥0.85). Out of 2335 cluster sets, 15 were significantly enriched for exoerythrocytic-stage active compounds (depicted above). GNF Malaria Box compounds are shown as circle nodes, and MMV Malaria Box compounds as square nodes. Active compounds are indicated in red and blue, for MMV and GNF compounds, respectively. Dark red/blue signifies IC_{50} < 1 µM, while light red/blue signifies IC_{50} < 10 µM. Inactive compounds are shown in black, and base scaffolds are shown in grey. It is important to note that of the 16 MMV compounds represented in the scaffold clustering, 13 of them were structurally identical to compounds also screened by the Novartis library using high-content imaging (TC=1).

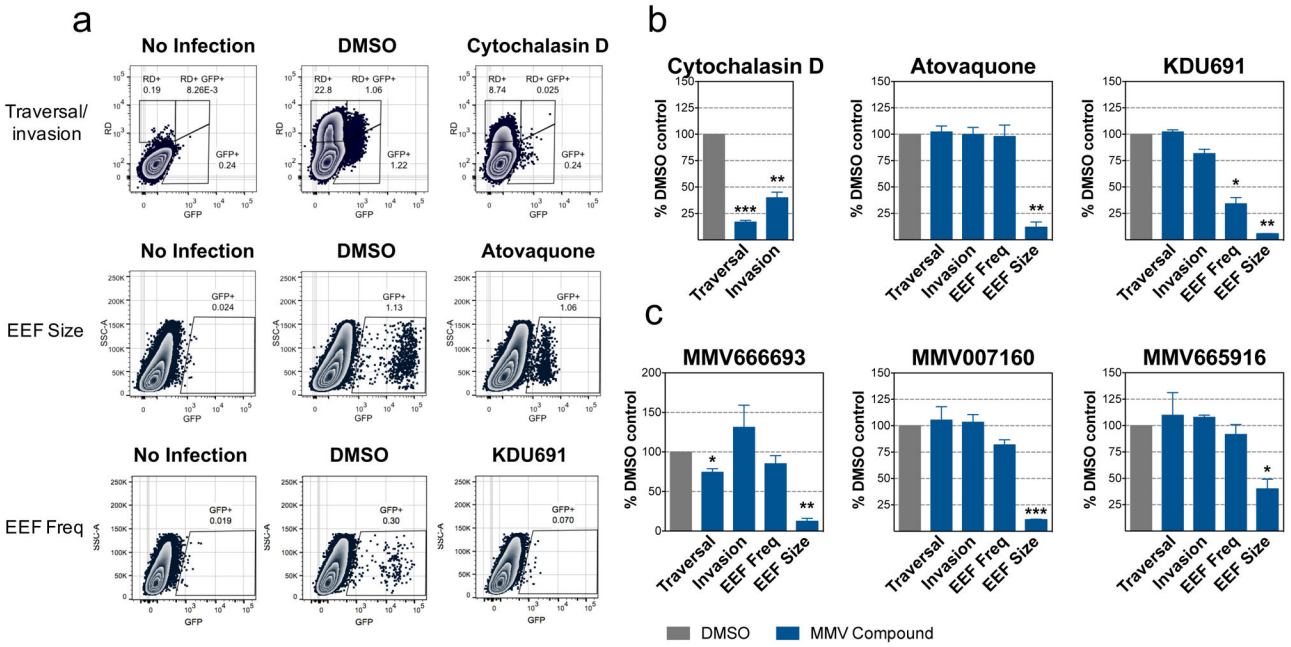

Figure 6. Validation of exoerythrocytic-stage activity using an established flow cytometry-based assay

a) Flow cytometry plots measuring traversal and invasion (at 2 hours post infection), and EEF frequency and development (at 48 hours post infection) of exoerythrocytic-stage malaria parasites in Huh7.5.1 cells as previously described for three of the most potent compounds. Cytochalasin D was used as a positive control for traversal and invasion, KDU691 was used as a positive control for EEF frequency, and atovaquone was used as a positive control for EEF frequency and development. While traversal was measured by the percentage of Rhodamine-dextran single-positive cells, invasion was measured by the percentage of Pb-GFP single-positive cells at 2 hours post infection. At 48 hours post infection, EEF frequency was measured by the percentage of Pb-GFP-positive cells, and EEF development was measured by the relative mean fluorescence intensity (MFI). Representative flow cytometry plots are shown. Atovaquone was tested at 1uM (due to slight cytotoxicity at 10 μM in Huh7.5.1 cells, (Figure S4), and Cytochalasin D and KDU691 was tested at 10 μM.

b) The mean and SEM are shown graphically from the traversal/invasion, EEF frequency, and EEF size control experiments shown in Figure 6a above (cytochalasin D, atovaquone, and KDU691, respectively). Values are normalized to the DMSO control.

c) Exoerythrocytic-stage traversal, invasion, EEF frequency, and EEF development are shown for MMV666693, MMV007160, and MMV665916. Mean and SEM from three replicate experiments are shown. MMV66693 was tested at 1 μM (due to slight cytotoxicity at 10 μM in Huh7.5.1 cells, (Figure S4), and MMV007160 and MMV665916 were tested at 10 μM.

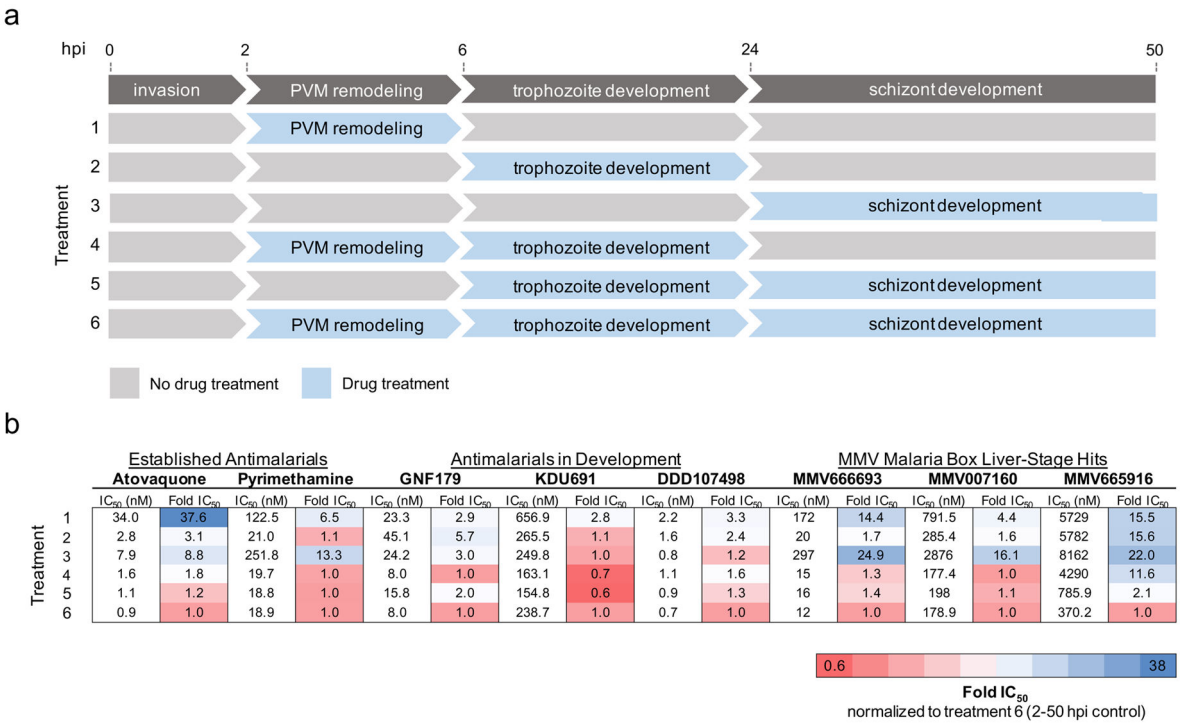

Figure 7. Exoerythrocytic-stage active compounds display unique potencies during exoerythrocytic-stage EEF development

a) Diagram illustrating the major stages of malaria parasite exoerythrocytic-stage development, including invasion, parasitophorous vacuole membrane (PVM) remodeling, trophozoite development, and EEF schizont development. During the first four hours after sporozoite invasion, the parasite dramatically remodels its parasitophorous vacuole membrane by degrading host cell-derived proteins and at the same time inserting its own parasite-derived proteins[(6)]. During the next 18 hours, the sporozoites transform from their elongated motile form to round, non-motile, and metabolically active trophozoites. The trophozoites undergo impressive nuclear replication starting at around 24 hours post infection, displaying one of the fastest replication rates known to eukaryotic organisms to develop into mature EEFs [(6)]. Drug treatments 1–6, corresponding to compound incubation during the exoerythrocytic developmental stages indicated, are shown.

b) Pb-Luc IC_{50} data for established antimalarial compounds (atovaquone and pyrimethamine), antimalarials in development (GNF179, KDU691, DDD107498), and the three MMV Malaria Box compounds (MMV666693, MMV007160, and MMV665916) added during Pb-Luc exoerythrocytic-stage development in a modified 384-well luciferase-based assay (discussed in Methods) are shown. Likewise, the Pb-Luc IC_{50} fold changes normalized to the 2–50 hour drug-treated controls are shown and colored based on the indicated heat map.